JOURNAL OF SPACECRAFT AND ROCKETS
Vol. 44, No. 3, May–June 2007

Earth–Moon Triangular Libration Point Spacecraft Formations

Kathryn A. Catlin* and Craig A. McLaughlin†
University of North Dakota, Grand Forks, North Dakota 58202-9008

DOI: 10.2514/1.20152

This paper presents a first investigation into the existence and nature of formation flight trajectories near the Earth–moon triangular libration points in the circular restricted three-body problem. Analytical equations of motion describing the relative dynamics within a rotating, lead-satellite-centered coordinate frame are derived from equations describing the absolute dynamics. Long-period and short-period trajectories of the relative motion are isolated, and parallel and leader–follower formations are designed for the long-period case. Results are compared to numerically integrated data: the total range error in all cases is less than 3% of the motion's maximum amplitude. Circular and projected circular formations are also described for the further simplified case of planar approximate motion based on the short-period regime. Formations are investigated to quantify their sensitivity to initial conditions. Potential effects of perturbing forces on the relative orbits are discussed, showing the solar point mass and solar radiation pressure to be significant, and Earth oblateness to be negligible.

Nomenclature

A_i, B_i	=	coefficients of solution to equations of motion
L_1, L_2, L_3	=	collinear libration points
L_4, L_5	=	triangular libration points
m_1, m_2	=	chief and deputy satellites in formation
$\boldsymbol{r}_r$	=	relative position vector of satellite 2 with respect to satellite 1
$\boldsymbol{r}_1, \boldsymbol{r}_2$	=	position vectors of satellites 1 and 2 with respect to libration point
$\boldsymbol{r}_{\oplus 1}$	=	vector from the Earth to satellite 1
s_1, s_2, s_z	=	dimensionless long-period, short-period, and out-of-plane frequencies for triangular libration point orbits: $s_{1,2} = (-(1/2)\{-1 \pm [1 - 27\mu(1-\mu)]^{1/2}\})^{1/2}$
t	=	nondimensional time, measured as an angle, rad
X, Y, Z	=	inertial barycentric coordinate frame
x, y, z	=	synodic barycentric coordinate frame
α	=	angle of rotation between synodic and principal coordinate systems; angular displacement of the semimajor axis of the ellipse of motion: $\tan 2\alpha = \sqrt{3}(1-2\mu)$
$\bar{\alpha}_1, \bar{\alpha}_2$	=	ratio of semiminor to semimajor axes of the ellipse of motion, for long and short periods, respectively: $\bar{\alpha}_{1,2} = (s_{1,2}^2 + \bar{\lambda}_2)/(2s_{1,2}) = (2s_{1,2})/(s_{1,2}^2 + \bar{\lambda}_1)$ where $\bar{\lambda}_{1,2} = (3/2)\{1 \pm [1 - 3\mu(1-\mu)]^{1/2}\}$
μ	=	mass parameter of the Earth–moon system; $\mu = \mu = 0.012150582$
ξ, η, ζ	=	synodic coordinate frame, centered on the libration point or the lead satellite
$\bar{\xi}, \bar{\eta}, \bar{\zeta}$	=	axis-aligned principal coordinate frame, centered on the libration point or the lead satellite

Subscripts

$r, 0$	=	subscripts denoting relative or initial state

Received 20 September 2005; revision received 5 November 2006; accepted for publication 28 November 2006.

*Graduate Student, Department of Space Studies, Campus Box 9008; currently Mission Planner/Orbital Analyst, Boeing Service Company, Leesburg, VA. AIAA Member.

†Assistant Professor, Department of Space Studies, Campus Box 9008. AIAA Senior Member.

I. Introduction

TRIANGULAR libration points have not previously been investigated with respect to their potential for formation flight missions. In this paper, relative equations of motion are developed and used to design several formation architectures at the Earth–moon triangular points, within the circular restricted three-body problem (CR3BP). The equations and formations developed are also applicable to missions about triangular points in other three-body systems.

Formation flying enables missions not possible with only a single satellite; the 2004 *Report of the President's Commission on Implementations of United States Space Exploration Policy* [1] recognized it as one of 19 technologies critical to the future of space exploration. An important factor is the reduction in design complexity. Each small satellite is considerably simpler than one large spacecraft needs to be, in turn reducing mission cost, complexity, and development time. Similarly, a critical failure in a spacecraft often forces a mission to abort, forfeiting both the objective and the investment of time and money that went into the project. Formation flight designs provide an increase in reliability; a failure in one member of a formation need not void the entire mission, as the cluster of satellites can continue to operate with reduced capabilities until a replacement can be launched, at lower cost than replacing either the entire formation or the single large spacecraft that would otherwise be employed. Thus critical maintenance and repair are made more economically feasible with formation flight, extending the lifetime of missions. For remote sensing or deep space imaging missions, not only does satellite formation flight increase the telescope's aperture size, but by making minor in-flight adjustments to the orbital parameters of the cluster, the aperture size, orientation, and optical constraints of the composite lens can be dynamically altered to observe a wide variety of objects and locations.

The collinear libration points of the sun–Earth/moon system have successfully served a number of missions. The International Sun–Earth Explorer-3 (ISEE-3, later renamed International Cometary Explorer) [2] was the first spacecraft to a libration point (sun–Earth/moon L_1) and the first to enter a halo orbit. Additional missions to the sun–Earth/moon L_1 libration point have included the Solar and Heliospheric Observatory (SOHO), the Advanced Composition Explorer (ACE), and Genesis [3]. In addition, the Wilkinson microwave anisotropy probe (WMAP) has flown about the sun–Earth/moon L_2 libration point. However, primarily because of the difficulty and expense in reaching the triangular points, no triangular points have yet been reached by a spacecraft; these points represent an untapped resource with potential to support space exploration activities of all types. The Earth–moon triangular points have similar advantages for remote sensing to those available at the sun–Earth/moon collinear points—an unobstructed view of deep space objects,

including the sun itself, and a location ideal for monitoring radiation and magnetic fields. Unfortunately, the cost of reaching the triangular points is significantly higher than reaching the collinear points. However, as more and more missions are developed that depend upon the availability of libration points for deep space and other remote sensing objectives, the Earth–moon triangular points may become attractive alternatives. The triangular points are also potential locations for eventual space stations and could serve as staging points for missions to the moon, the outer planets and asteroids, and beyond. For these reasons, not only are the Earth–moon triangular libration points good settings for missions in their own right, they may also serve as test bed and technology demonstration locations for missions and hardware that will eventually be in use at libration points in other areas of the solar system. In particular, a mission to one or both of the Earth–moon triangular libration points would be able to provide invaluable support—as a communications relay, supply depot, etc.—for any long-term human mission to the moon or Mars. Farquhar [4] provides an excellent bibliography in a special issue of *The Journal of the Astronautical Sciences* on libration point mission design and analysis for single spacecraft.

The sun–Earth/moon collinear points have so far been the most studied and used of the libration points, both for single craft and formation flight missions. Segerman and Zedd [5] used the circular restricted three-body problem to develop both analytical and nonlinear solutions for both hub and telescope motion of a six-spacecraft telescope formation [specifically the microarcsecond x-ray imaging mission (MAXIM) Pathfinder]. Collange and Leitner [6] studied the relative motion of two spacecraft near the sun–Earth L_1 point, developing and testing conditions that satisfy a Lissajous trajectory around the L_1 point for both satellites, whose orbit around each other is then a similar, smaller Lissajous trajectory. They applied formation design to their analysis, describing the stability and relative efficiency of circular and projected circular formations in both Lissajous and halo orbits of two spacecraft around L_1. Howell and Marchand [7] provide a summary of collinear libration point formation flying work and discuss natural and nonnatural spacecraft formations near the sun–Earth/moon L_1 and L_2. Marchand and Howell [8] present control strategies and propulsion requirements for libration point formation flying missions. Vadali et al. [9] described several satellite formations using halo orbits at the sun–Earth/moon L_1, intended for use in telescope interferometry. And in a series of papers, Luquette and Sanner [10,11] described the development of linearized dynamics of relative motion of two spacecraft at the sun–Earth/moon L_1 point within the restricted three-body problem. Luquette et al. [12] later extended the analysis to provide linearized dynamics for relative motion within the n-body problem, with specific application to motion around L_1, providing a basis for libration point formation control within any n-body gravitational field.

The majority of work in the field of triangular libration point research exists with the intent of quantifying the existence and stability of orbits about the points within the Earth–moon system. Most of the literature remains deeply rooted in the circular restricted three-body problem. Michael [13] and Szebehely [14] provide comprehensive descriptions of the equations of motion of a single object near the equilateral points within the CR3BP. In an alternative approach, Rand and Podgorski [15] derived time-independent polar equations of motion to describe periodic orbits around L_4 in the CR3BP. Blackburn et al. [16] used computerized numerical integration techniques to find bounded, quasiperiodic orbits around the CR3BP L_4 point. McKenzie and Szebehely [17] determined the region about each triangular point within which a particle traveling at zero initial velocity will orbit the libration point indefinitely.

Several simple alterations have been proposed to the CR3BP methodology, to correct for some limited perturbing effects and bring the model closer to an accurate representation of the real world. Szebehely [18], for example, proposed a unique method to correct for the lunar eccentricity with a "pulsating" coordinate system and remarked that the accuracy of physical constants used in the calculations has a large influence on the projected orbit. In the Earth–moon system, the perturbation of greatest concern is that caused by the effect of the sun's gravity on the infinitesimal third body. Incorporating solar gravity requires solution of a three-plus-one-body problem, or restricted four-body problem (R4BP). It is well known that these equations are not analytically solvable; however, many researchers have studied various simplified models of the R4BP. In one of the earliest such reports, Danby [19] remarked that with the inclusion of solar gravity and radiation forces, the triangular points cease to be equilateral, and their stability is called into severe question. Indeed, his analysis showed that while for certain conditions, the triangular points may be stable as indicated by the simplified Lagrangian analysis, for most true situations the triangular points are actually dynamically unstable. He stressed that to address the question, nonlinear analyses are required. Breakwell and Pringle [20], among others, however, numerically investigated the four-body problem and discovered generally stable libration point orbits in near resonance with the motion of the three primaries.

Although the collinear libration points have attracted considerable interest for formation flight missions, very little research exists in the literature describing the dynamics of formation flight at the triangular points. Gurfil and Kasdin [21] described the existence of stable formations, with bounded relative position, within the CR3BP for the sun–Earth system. They also developed a time-varying control law for maintenance of these formations, which is applicable to any deep space location governed by the CR3BP, not just those in the vicinity of libration points. Gómez et al. [22] provide a bibliography on the dynamics and mission design near the triangular libration points as well as cover the fundamentals of analysis near the points. In addition, they performed a preliminary analysis of relative motion near the triangular points, intending to investigate the possibility of dust clouds congregating near the points, as well as the prospects for satellite formation flight. They found the variation in relative vectors, particularly the relative velocity vectors, to be quite large, but they did discover some periodic relative trajectories. In a follow-up volume, Gómez et al. [23] provide more advanced techniques and analysis on missions near the triangular libration points.

The triangular libration points have been the subject of considerable scrutiny and analysis in an effort to comprehend the extremely complex dynamics of their spatial location. All analyses are to some degree idealized and simplified; although some models come close, no investigation has yet provided real-world accurate descriptions of motion around or near the Earth–moon triangular points. Specifically, only very limited investigations into formation flight at triangular libration points have been performed. This research intends to provide additional analysis of the potential for formation flight at the triangular points within the simplified constraints of the circular restricted three-body problem. Once the analytical model has been obtained, it can be used to develop initial descriptions of the motion, preliminary to a more comprehensive numerical nonlinear verification and analysis. In addition, the linear solutions can be used to seed more complex nonlinear solutions.

Although fast and accurate numerical methods exist to fully describe motion at the triangular points, derivation of a linearized analytical model of relative motion is helpful for formation design. Other advantages include a better understanding of the forces involved, and avoiding the errors from numerical methods that might go unnoticed without an analytical basis on the part of the researcher. This paper provides the first analytical approach to describe the relative motion of spacecraft near triangular libration points, with particular emphasis on formation flight, and a first look at the relative perturbation environment near the triangular libration points in the Earth–moon system. The focus is on the Earth–moon triangular libration points, but should be even more applicable to other triangular libration points in the solar system because they have a more benign perturbation environment.

II. Approach

A. Relative Motion

Previous work by the authors [24] discussed the development of relative equations of motion for spacecraft near the Earth–moon L_4

point within the CR3BP, using a dimensionless synodic coordinate system, centered at the Earth–moon barycenter and aligned with the axis connecting the Earth and the moon. The Earth is aligned with the positive x axis and the L_4 point is located above that axis, trailing the moon in its orbit (Fig. 1). Time is nondimensionalized with a multiplication by the mean motion of the moon. Normalization is achieved by setting the distance between the Earth and moon equal to 1. A mass parameter μ is defined for each primary body, equal to its mass divided by the sum of both masses; the sum of these two mass parameters is equal to 1. The mass parameter and frequencies can be calculated directly, or looked up in a table. For the Earth–moon system, the mass parameter used in this paper is $\mu = 0.012150582$, obtained from the Swingby integration software (see below). This value of μ is consistent with that given by Dunham and Muhonen [25]. For this nondimensional case, the out-of-plane frequency (s_z) is equal to 1. Because the two-body equations of motion intrinsically link mass to distance, the entire problem can be described in terms of a single dimensionless mass parameter, that of the moon, as shown in Fig. 1. Szebehely [14] provides a detailed derivation of the two-dimensional linearized equations of motion for the third body within this coordinate system.

To study the motion of a spacecraft around the L_4 point, Szebehely [14] defines a second coordinate system, analogous to the synodic system but centered at L_4. The equations of motion are moved into this new coordinate system by expanding the force function about L_4 and excluding higher order terms. The equations are further simplified by rotating this second coordinate system to align with the principal axes of the ellipse of motion.

The equations of motion of one satellite with respect to another will be referred to as the relative equations of motion in this paper. The development of the relative equations of motion, first presented in [24], starts with Szebehely's method for determining the position of a single satellite in orbit around the L_4 triangular libration point. Now, posit the presence of a second satellite, also orbiting L_4, and flying in formation with the first (Fig. 1). The problem is to find equations describing the relative motion of the second satellite with respect to the first, in terms of a coordinate system analogous to the principal frame but centered at the leading satellite (satellite 1) (Fig. 1, inset). The relative position can be found by subtracting the location of the first satellite from that of the second:

$$\bar{\xi}_r = \bar{\xi}_2 - \bar{\xi}_1 \qquad \bar{\eta}_r = \bar{\eta}_2 - \bar{\eta}_1 \qquad \bar{\zeta}_r = \bar{\zeta}_2 - \bar{\zeta}_1 \tag{1}$$

Differentiating twice yields

$$\ddot{\bar{\xi}}_r = \ddot{\bar{\xi}}_2 - \ddot{\bar{\xi}}_1 \qquad \ddot{\bar{\eta}}_r = \ddot{\bar{\eta}}_2 - \ddot{\bar{\eta}}_1 \qquad \ddot{\bar{\zeta}}_r = \ddot{\bar{\zeta}}_2 - \ddot{\bar{\zeta}}_1 \tag{2}$$

Note that the centripetal, tangential, and Coriolis accelerations are inherent in the equations for $\ddot{\bar{\xi}}_{1,2}$, $\ddot{\bar{\eta}}_{1,2}$, and $\ddot{\bar{\zeta}}_{1,2}$.

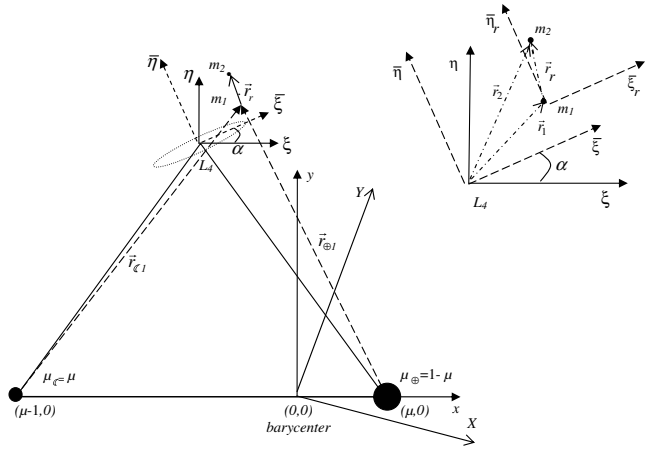

Fig. 1 Coordinate systems. The dotted ellipse corresponds to long-period global motion about the libration point. The inset shows the coordinate system for relative motion. Out-of-plane motion (Z, z, ζ, ζ_r) is positive out of the page. Not to scale.

From the equations for a single satellite L_4 (Szebehely [14]):

$$\begin{aligned} \ddot{\bar{\xi}}_2 &= 2\left(\dot{\bar{\eta}}_1 + \dot{\bar{\eta}}_r\right) + \bar{\lambda}_2\left(\bar{\xi}_1 + \bar{\xi}_r\right) \\ \ddot{\bar{\eta}}_2 &= -2\left(\dot{\bar{\xi}}_1 + \dot{\bar{\xi}}_r\right) + \bar{\lambda}_1\left(\bar{\eta}_1 + \bar{\eta}_r\right) \qquad \ddot{\bar{\zeta}}_2 = -\left(\bar{\zeta}_1 + \bar{\zeta}_r\right) \end{aligned} \tag{3}$$

a substitution can be quickly performed such that the position and velocity of satellite 1 drop out of Eq. (3), leaving us with

$$\ddot{\bar{\xi}}_r - 2\dot{\bar{\eta}}_r = \bar{\lambda}_2\bar{\xi}_r \qquad \ddot{\bar{\eta}}_r + 2\dot{\bar{\xi}}_r = \bar{\lambda}_1\bar{\eta}_r \qquad \ddot{\bar{\zeta}}_r = -s_z^2\bar{\zeta}_r \tag{4}$$

equations of motion in the same form as the relative motion of one satellite about L_4. The form of the eigenvalues, which depend solely on μ, is unchanged. Therefore, the general solution to the equations of relative motion for two satellites around the Earth–moon L_4 point is of the same form as the solution for a single satellite relative to the libration point. The equations of relative motion then become

$$\begin{aligned} \bar{\xi}_r &= A_1\cos s_1 t + B_1\sin s_1 t + A_2\cos s_2 t + B_2\sin s_2 t \\ \bar{\eta}_r &= \bar{A}_1\cos s_1 t + \bar{B}_1\sin s_1 t + \bar{A}_2\cos s_2 t + \bar{B}_2\sin s_2 t \\ \bar{\zeta}_r &= \bar{\zeta}_{r_0}\cos s_z t + \frac{\dot{\bar{\zeta}}_{r_0}}{s_z}\sin s_z t \end{aligned} \tag{5}$$

where

$$A_1 = \bar{\xi}_{r_0} - \frac{2}{s_1^2 - s_2^2}\left(\dot{\bar{\eta}}_{r_0} + \bar{\alpha}_1 s_1 \bar{\xi}_{r_0}\right)$$

$$A_2 = \frac{2}{s_1^2 - s_2^2}\left(\dot{\bar{\eta}}_{r_0} + \bar{\alpha}_1 s_1 \bar{\xi}_{r_0}\right)$$

$$B_1 = \frac{1}{s_1}\dot{\bar{\xi}}_{r_0} - \frac{s_2}{s_1(\bar{\alpha}_2 s_1 - \bar{\alpha}_1 s_2)}\left(s_1\bar{\eta}_{r_0} - \bar{\alpha}_1\dot{\bar{\xi}}_{r_0}\right)$$

$$B_2 = \frac{1}{(\bar{\alpha}_2 s_1 - \bar{\alpha}_1 s_2)}\left(s_1\bar{\eta}_{r_0} - \bar{\alpha}_1\dot{\bar{\xi}}_{r_0}\right) \qquad \bar{A}_1 = \bar{\alpha}_1 B_1$$

$$\bar{A}_2 = \bar{\alpha}_2 B_2, \qquad \bar{B}_1 = -\bar{\alpha}_1 A_1, \qquad \bar{B}_2 = -\bar{\alpha}_2 A_2$$

For definition of parameters not explicitly calculated in the text, refer to the nomenclature section. Velocities are obtained by differentiation. These equations have the same form as the equations of an object moving with respect to the triangular libration point within the CR3BP, but the sizes of the relative motion will be smaller.

When including both long- and short-period terms (s_1 and s_2), the relative dynamics resolve into intricate three-dimensional curves. The axis ratio is approximately 16/5 and the period is 458 days. Although mathematically interesting, practically speaking these orbits are too complex to be ideal for most spacecraft formation applications. If one of the periods can be eliminated, the motion will become purely elliptical and more applicable to formation flight missions because the second satellite will have repeatable, periodic motion with respect to the first satellite. Fortunately, either period is easily eliminated by judicial selection of the initial velocity conditions. To eliminate the short period (i.e., to obtain only long-period motion) the initial velocity conditions are

$$\dot{\bar{\xi}}_{r0} = \frac{\bar{\eta}_{r0} s_1}{\bar{\alpha}_1} \qquad \dot{\bar{\eta}}_{r0} = -\bar{\xi}_{r0} s_1 \bar{\alpha}_1 \tag{6}$$

To eliminate the long period (i.e., to obtain only short-period motion) the initial velocity conditions are

$$\dot{\bar{\xi}}_{r0} = \frac{\bar{\eta}_{r0} s_2}{\bar{\alpha}_2} \qquad \dot{\bar{\eta}}_{r0} = -\bar{\xi}_{r0} s_2 \bar{\alpha}_2 \tag{7}$$

The initial out-of-plane (ζ) velocity is unconstrained.

Thus, when substituting Eq. (6) into Eq. (5), the relative dynamics for long-period motion are of the form

$$\bar{\xi}_r = \frac{\bar{\eta}_{r0}}{\bar{\alpha}_1}\sin s_1 t + \bar{\xi}_{r0}\cos s_1 t \qquad \bar{\eta}_r = \bar{\eta}_{r0}\cos s_1 t - \bar{\alpha}_1\bar{\xi}_{r0}\sin s_1 t$$

$$\bar{\zeta}_r = \bar{\zeta}_{r0}\cos s_z t + \frac{\dot{\bar{\zeta}}_{r0}}{s_z}\sin s_z t \tag{8}$$

Again, velocities are obtained by differentiating once. For a model containing only the short-period terms, the ratio of semimajor to semiminor axes $(1/\bar{\alpha}_2)$ is approximately 2, and the period is approximately one month; for long-period motion, the ratio $(1/\bar{\alpha}_1)$ is close to 16/3, and the period is close to 92 days. Under these conditions, the initial relative velocity is constrained and small, on the order of millimeters per second for the initial positions investigated, keeping the shape of the orbit small in comparison to the dual-period case.

Analytical results developed in this paper are compared to numerically integrated data from Swingby release 2002–01, a mission analysis and trajectory design system developed at NASA's Goddard Space Flight Center. Swingby's coordinate system uses an alternate libration point numbering scheme; the L_4 point leads rather than trails the moon in its orbit around the Earth. Therefore, within Swingby the simulation is run in an L_5-centric frame; initial conditions are rotated first from the "bar" frame through an angle of α to place them in Swingby's frame, then results of the integration are rotated back through the negative angle for comparison with the analytical model. Swingby does not automatically model relative motion; instead, the relative trajectory is found by subtracting the position of satellite 1 from the position of satellite 2 before performing the rotation back to the principal coordinate system. To simulate motion within the circular restricted three-body problem, all perturbations except the Earth and the moon as point masses are turned off in the propagation configurations, which is a Runge–Kutta–Nystrom integration about the Earth, with a time step of 0.5 days. A shorter time step of 0.05 days was also tried in each case and did not result in an improvement in the simulation. Running the integration with respect to the libration point or the moon revealed an error in the Swingby code, which fails to correctly apply the effects of the gravity of the Earth and the moon in those cases, so the Earth was selected as the central body of the integration. Within the universe, the position of the moon is computed analytically via the two-body method in a circular orbit about the Earth, with all initial Keplerian elements set to zero except the semimajor axis. The Earth's position is not calculated and assumed to be fixed in space.

B. Formation Design

Within this relative dynamic framework, formations are designed by judiciously selecting the initial conditions, beyond the constraints in Eqs. (6) and (7), to generate a desired relative motion. The first of these is the parallel formation.

In the parallel, or in-plane, formation, all satellites in the cluster have the same out-of-plane component at all times, but are offset in the in-plane (ξ and η) directions. The initial conditions are otherwise identical. This is equivalent to the introduction of a phase shift, as shown in Fig. 2. Figure 3 illustrates the planar nature of the formation. The Swingby results will be discussed in the Results section. Viewed from the plane of motion, the parallel formation appears similar to the leader–follower formation. Indeed, at time $t+1$, satellite 2 occupies the same ξ and η coordinates that satellite 1 had at time t; however, both satellites are constrained to share the same ζ coordinate.

The leader–follower formation, as its name implies, consists of one satellite following another on exactly the same orbital path. The formation is achieved by setting the position of satellite 2 at time 1 equal to the position of satellite 1 at time 2. This requires knowledge of the future position of satellite 1. Effectively, this calculation results in a formation in which satellite 1 is in fact following satellite 2. However, this is simply a matter of nomenclature and does not make a difference in the formation's appearance or applicability.

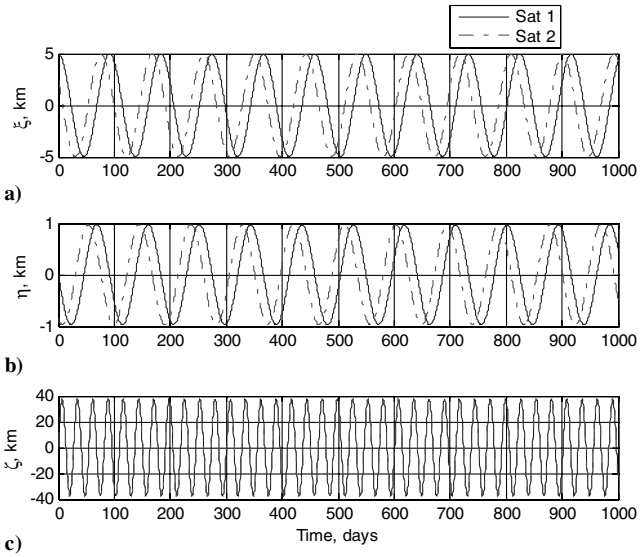

Fig. 2 Absolute motion of two spacecraft in a parallel formation about L_4. a), b) Note the phase shift evident in the in-plane components ξ and η. c) The out-of-plane components for satellites 1 and 2 are identical.

Figure 4 shows the leader–follower nature of the formation, and Fig. 5 shows the two- and three-dimensional relative motion.

One of the most useful and often discussed satellite formations in Earth orbit is the circular formation, in which satellites maintain a constant relative distance from one another. This results in a formation that, within the satellite reference frame, resembles a circle or sphere with the leading satellite at its center. The natural circular formation, however, turns out to be impossible to achieve for long-period motion at L_4; all long-period motion, relative as well as absolute, about L_4 occurs in an in-plane elliptical orbit with the ratio of semimajor to semiminor axes of approximately 16/3. To achieve a circular formation, this ratio would need to equal 1, or the out-of-plane frequency would need to equal the frequency of the in-plane motion to allow the plane of relative motion to stretch. At collinear libration points, a planar approximation can be made equating the single in-plane frequency with the out-of-plane frequency, and allowing circular formations to be achieved (see [6]). For long-period motion at triangular points, s_z is not sufficiently close to s_1 to permit such an approximation.

However, if one considers the short-period motion about L_4, circular formations become more feasible. The short-period

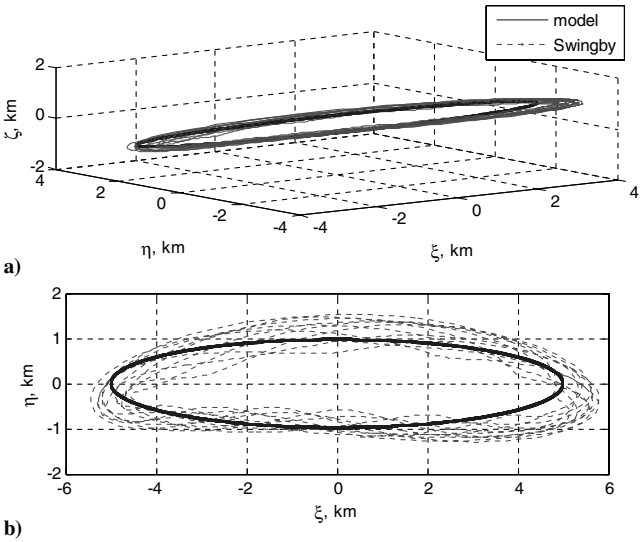

Fig. 3 Relative motion of satellite 2 with respect to satellite 1 in parallel formation about L_4 over 1000 days. a) Three-dimensional relative motion. Note that the out-of-plane component is not to scale. b) In-plane relative motion.

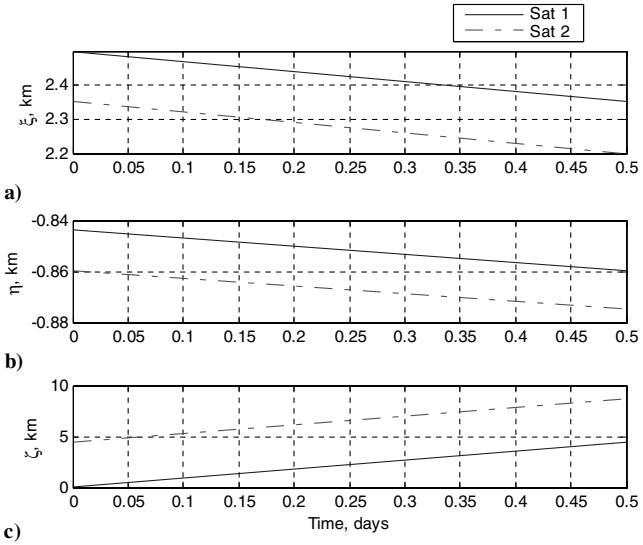

Fig. 4 Absolute motion of two spacecraft in leader–follower formation at L_4 over one time step for a),b) in-plane and c) out-of-plane motion. Note satellite 1 follows exactly 0.5 days behind satellite 2.

frequency s_2 differs from s_z by less than 0.05 nondimensional frequency units, so a planar approximation can be made by artificially setting s_2 equal to 1 (the nondimensionalized out-of-plane frequency). Also setting $\bar{\eta}_0 = 0$, the resulting equations are

$$\bar{\xi} = \bar{\xi}_0 \cos s_2 t \qquad \bar{\eta} = -\bar{\alpha}_2 \bar{\xi}_0 \sin s_2 t$$
$$\bar{\zeta} = \bar{\zeta}_0 \cos s_z t + \frac{\dot{\bar{\zeta}}_0}{s_z} \sin s_z t \tag{9}$$

where $s_2 = s_z = 1$. Applying the circular constraint to Eq. (9), the required initial relative conditions for a circular formation are

$$\bar{\xi}_o = \bar{\xi}_o \qquad \dot{\bar{\xi}}_o = 0 \qquad \bar{\eta}_0 = 0 \qquad \dot{\bar{\eta}}_0 = -\bar{\xi}_0 s_2 \bar{\alpha}_2 \qquad \bar{\zeta}_0 = 0$$
$$\dot{\bar{\zeta}}_0 = \pm \bar{\xi}_0 \sqrt{(1 - \bar{\alpha}_2^2)} \tag{10}$$

This results in a circle, tilted along the η axis through an angle of $\pm\cos^{-1}\bar{\alpha}_2$, approximately 60 deg for the Earth–moon system. These dynamics are not an accurate representation of the real motion, even within the CR3BP, because they require an artificial substitution of 1

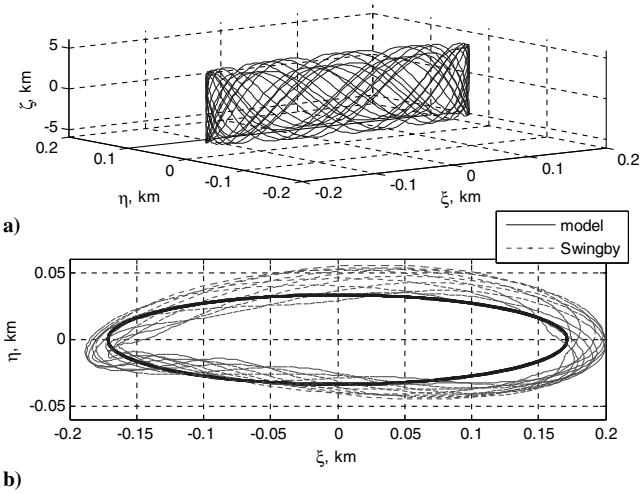

Fig. 5 Relative motion of satellite 2 with respect to satellite 1 in leader–follower formation at L_4 over 1000 days. a) The three-dimensional relative motion. Note that the out-of-plane component is not to scale and that most of the motion is out of plane. b) The in-plane motion including Swingby results.

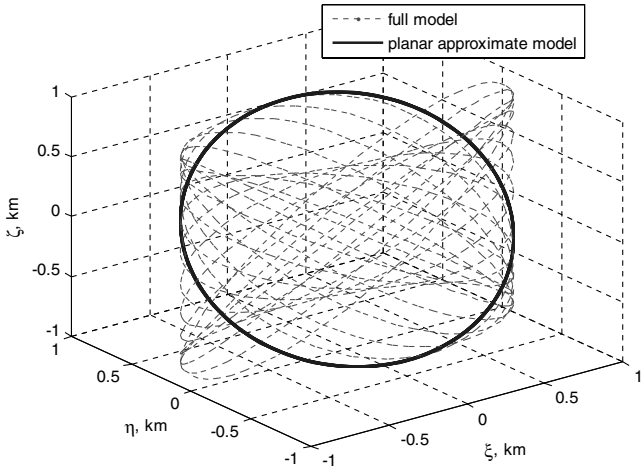

Fig. 6 Relative motion of satellite 2 with respect to satellite 1 in circular formation at L_4 showing the inaccuracy of the planar approximation.

for the short-period frequency; but they can be used to gain an understanding of the motion available, and perhaps to approximate circular analogous formations within the CR3BP. One possible way in which the circular formation might be put to use is to take each period of the orbit as a separate entity, feeding the model new initial conditions at the beginning of each orbit. The circularity of the relative orbit would not hold constant over the entire mission lifetime, but it would be approximately constant over each month-long period. Thrust could also be applied at the end of each period to reset the spacecraft on the desired particular circular relative orbit. Refer to Fig. 6 for a graphical interpretation of the difference between planar approximate and CR3BP models of the circular formation. It is evident that the planar approximate model is not nearly sufficient to describe the motion, not even the CR3BP case, and additional control will be required to maintain a circular formation.

Another related formation often used in Earth-orbiting clusters is the projected circular formation. In this formation, the satellites do not maintain a constant distance from one another, but when the motion is projected onto a specified plane, it appears circular. It is similar to the circular formation in that it is achieved by rotating the plane of motion with respect to one or more of the axes, such that the resulting trajectory appears circular when viewed from a specified pointing direction: indeed, the circular formation is a special case of the projected circular formation. Again, because the ability to point is dependent on motion confined to a single plane, a planar motion approximation is required. This remains infeasible for the long-period case. For the short-period case, however, the planar approximation still approximately holds, and planar elliptical orbits can be developed for a wide range of pointing directions by adjusting the $\bar{\eta}$ and $\bar{\zeta}$ values from Eq. (10). It must again be emphasized that in the real world, the planar approximation requires setting the short-period frequency equal to 1, a false assumption, and therefore does not provide an accurate representation of the dynamics. However, similar to the circular formation, an approximate projected circular formation could be maintained within the CR3BP by the application of periodic thrust. Such an orbit could be useful for observation and remote sensing: a distributed telescope formation could be pointed at the Earth, moon, sun, or other body of interest.

III. Results

A. Simulations

Table 1 contains the initial absolute (with respect to the libration point) and relative (with respect to satellite 1) positions for each of the six cases: dual-period, long-period, short-period, parallel formation, leader–follower formation, and circular formation. In all cases satellite 1 is on a long-period ellipse with respect to the libration point. This is not a necessary constraint, but was convenient for comparison in this section. The formations describe the relative motion of satellite 2 with respect to satellite 1. Initial conditions are

Table 1 Initial conditions

	$\bar{\xi}_0$, km	$\bar{\eta}_0$, km	$\bar{\zeta}_0$, km	$\dot{\bar{\xi}}_0$, mm/s	$\dot{\bar{\eta}}_0$, mm/s	$\dot{\bar{\zeta}}_0$, mm/s
Dual-periodic case						
Satellite 1	5	2	1	10,000	10,000	100
Satellite 2	4	3	0.1	15,000	0	110
Relative	−1	1	−0.9	5,000	−10, 000	10
Long-period case						
Satellite 1	5	2	1	8.149	−0.7731	100
Satellite 2	4	3	0.1	12.22	−0.6185	110
Relative	−1	1	−0.9	4.075	0.1546	10
Short-period case						
Satellite 1	5	2	1	10.34	−6.244	100
Satellite 2	4	3	0.1	15.51	−4.995	110
Relative	−1	1	−0.9	5.169	1.249	10
Parallel formation						
Satellite 1	5	0	0.001	0	−0.7732	100
Satellite 2	2.5	−0.8435	0.001	−3.437	−0.3866	100
Relative	−2.5	−0.8435	0	−3.437	0.3866	0
Leader–follower formation						
Satellite 1	2.5	−0.8435	0.1	−3.437	−0.3866	100
Satellite 2	2.350	−0.8597	4.410	−3.503	−0.3634	99.31
Relative	−0.1499	−0.01620	4.310	−0.06601	0.02318	−0.6909
Circular formation						
Satellite 1	5	0	0	0	−6.700	−11.50
Satellite 2	4	0	0	0	−5.360	−9.199
Relative	−1	0	0	0	1.340	2.300

Table 2 Errors

	ξ, m	η, m	ζ, m	Total separation, m	$\dot{\xi}$, μm/s	$\dot{\eta}$, μm/s	$\dot{\zeta}$, μm/s	Total velocity, μm/s
Dual-period case								
Average error	−1655	524.3	−0.2361	−2269	−0.1814	0.04497	$2.917e-5$	0.5508
Percent error	4.37	4.65	6.11	0.59	0.34	0.22	0.28	1.04
Long-period case								
Average error	−584.0	211.0	31.35	−149.9	−0.003186	$8.839e-4$	0.01487	−0.03607
Percent error	11.17	20.70	0.81	2.321	0.08	0.11	0.14	0.32
Short-period case								
Average error	−56.88	−16.28	31.15	37.16	−0.03164	−0.01071	0.01487	0.04326
Percent error	2.51	1.46	0.81	0.83	0.55	0.38	0.14	0.37
Parallel formation								
Average error	508.6	−183.2	0.007796	129.4	0.003512	−0.002385	$-4.308e-7$	0.2037
Percent error	10.17	18.81	N/A	2.59	0.09	0.31	N/A	5.13
Leader–follower formation								
Average error	9.992	−3.610	9.384	−4.370	0.05765	−0.02275	−9.887	−14.97
Percent error	5.82	10.81	0.22	0.133	0.04	0.09	0.09	0.13
Circular formation (CR3BP approximation)								
Average error	11.62	−1.572	6.355	66.56	3.069	−7.746	1.121	157.8
Percent error	1.16	0.32	0.73	5.02	0.12	0.62	0.05	4.59

provided in the rotated (bar) coordinate frame; a rotation of the initial conditions is required to obtain the presented Swingby results. The parallel and leader–follower formations are modeled for the long-period relative motion case, the circular for the short-period relative motion case. The dual-, long-, and short-period cases are modeled over 458 days; the formations are modeled over 1000 days. Errors were obtained by subtracting the analytically modeled value from the numerical value. Percentage errors were then calculated by dividing the average error by the maximum amplitude of the model curve. Average and percentage errors for all cases are summarized in Table 2; average errors are rounded to four figures and percentages to hundredths of a percent. The highest errors in total position and velocity were found for the parallel formation, with a total position error of 2.6% or 130 m, and total velocity error of 5.13%, or 0.2 μm/s.

In the interest of space, only representative plots from each case are provided. Both absolute and relative motion of the formations, for both the modeled and Swingby cases, were shown previously in Figs. 2–6. Figure 7 shows the in-plane relative position of two spacecraft for the case including both frequencies; Fig. 8 shows the difference in the magnitude of the relative position vector for this

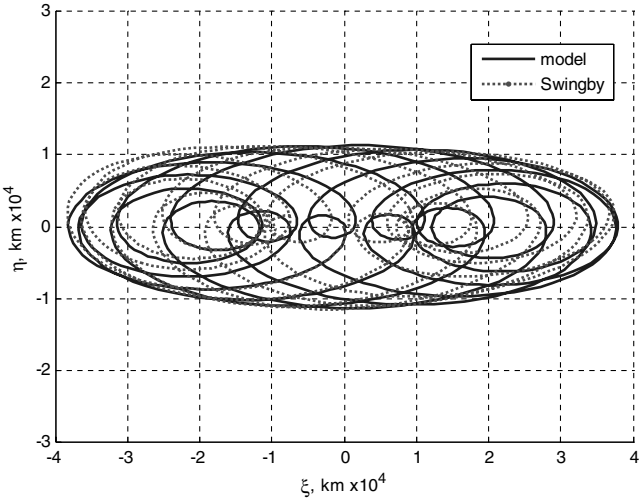

Fig. 7 In-plane relative position over 458 days for two satellites at L_4 for the dual-periodic case.

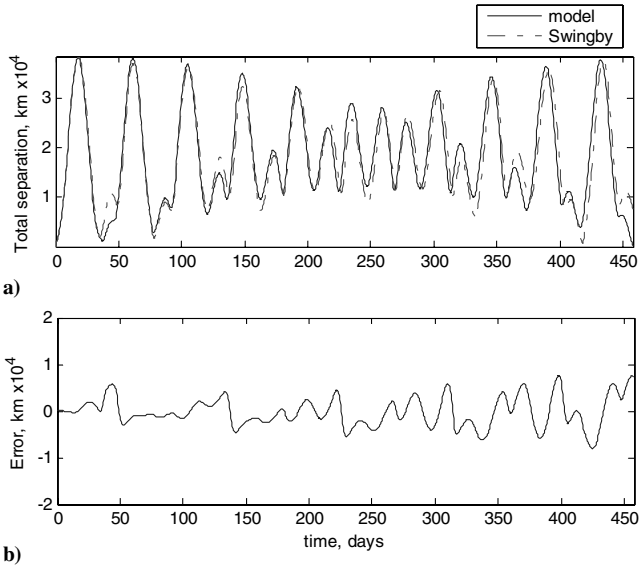

Fig. 8 Comparison of the magnitude of the relative position vector of two satellites at L_4 with the Swingby model for the dual-periodic case. a) Total separation; b) error in model.

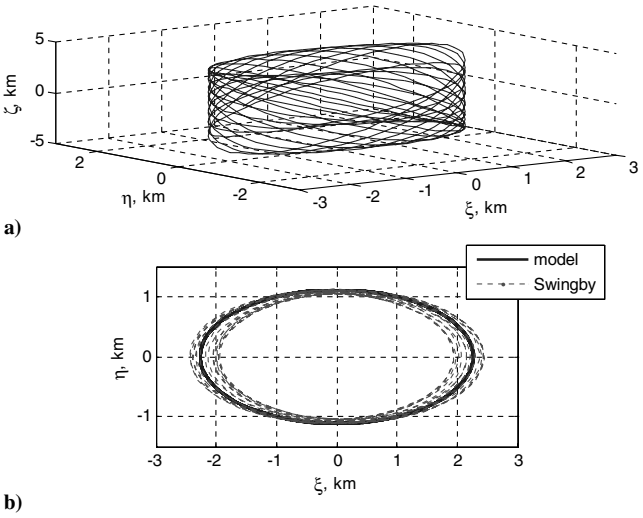

Fig. 9 Relative motion of satellite 2 with respect to satellite 1 near Earth–moon L_4 over 458 days: short-periodic case. a) Three-dimensional case. Note the out-of-plane relative motion is not to scale and is larger than the in-plane relative motion. b) In-plane relative motion with Swingby results included.

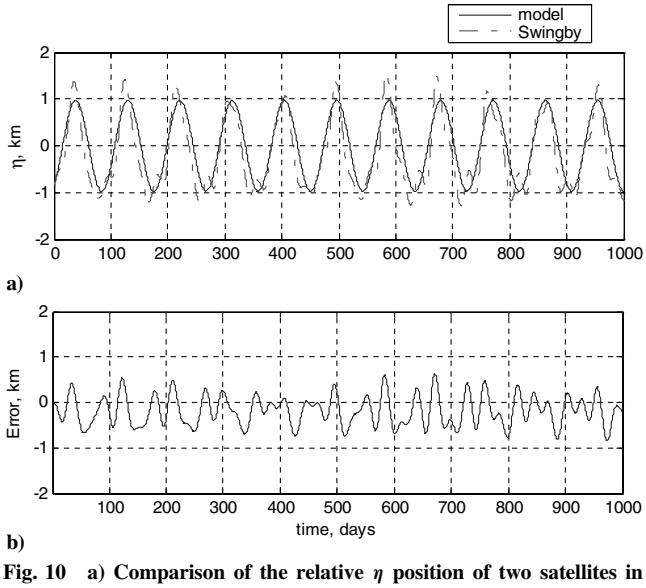

Fig. 10 a) Comparison of the relative η position of two satellites in parallel formation at L_4 with Swingby. b) Error in the analytical solution.

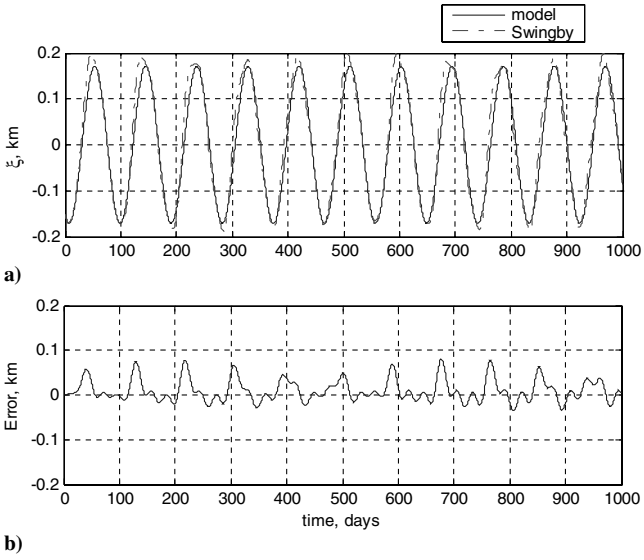

Fig. 11 a) Comparison of the relative ξ position of two satellites in leader–follower formation at L_4 with Swingby. b) Error in the analytical model.

dual-period case between the analytical model and the Swingby simulation. Figures 3 and 5 show examples of the long-period relative motion, and Fig. 9 illustrates the short-period relative motion and the difference from the Swingby simulation. Figures 10 and 11 are representative comparisons between modeled and Swingby data for components of the relative position vector for the parallel and leader–follower formations, respectively. Plots are shown in the rotated (bar) reference frame.

B. Sources of Error

It is clear from the previous plots that at least one source of error must be present between the analytical model and the Swingby simulation. Remnants of long-period motion are evident in the simulated short-period case, and vice versa; in the dual-period case, an unexpected, secondary longer period is evident in the ζ direction. There is also a slight phase shift apparent over the course of the simulation. These errors are primarily due to Swingby's use of nonlinear equations of motion in its dynamical model; the derived analytical model is linear, and the remaining nonlinear terms in Swingby cause the lingering small periodic discrepancy. All forces that can be turned off in Swingby have been removed. Similarly any possible error sources due to lunar eccentricity or inclination, or noncircularities in the Earth's orbit around the sun, are removed in the Swingby universe configuration, and the mass ratio is the same in both the model and the Swingby. It is possible that the discrepancies are caused by a dilution of precision of initial conditions during the coordinate transformation and subsequent manual input to Swingby. Despite these errors, the model results are sufficiently close to the simulated trajectories to provide assurance that the model is a good first-order approximation of the relative motion.

C. Sensitivity to Initial Conditions

It is the intent of this sensitivity analysis to determine what degree of error in initial conditions will continue to result in the desired trajectory: in other words, how much precision is required in the orbital insertion stage of a mission to ensure that the spacecraft formation remains intact. For long- and short-period formations, the critical values to maintain that periodicity are the initial relative

Table 3 Sensitivity to initial conditions. Positions are given in meters; velocities in millimeters per second

	Long period	Short period	Parallel	Leader–follower	Circular	Circular (planar approx.)
Error in initial position						
<10% relative position error						
%	1.2434	1.005	10.01	2.955	0.1493	0.1520
Initial position	62.18	50.27	264.2	78.01	7.613	7.751
Initial velocity	1.248	1.012	10.02	2.936	0.02799	0.02904
Relative initial position	20.84	16.85	264.2	127.4	1.493	1.520
Relative initial velocity	0.1343	0.1138	0.3463	0.02052	0.003931	0.004046
Formation maintenance (<10 m)						
%	——	——	1000	0.04760	——	0.01520
Initial position	——	——	2639	1.257	——	0.7751
Initial velocity	——	——	1000.6	0.047301	——	0.002904
Relative initial position	——	——	26,384	2.053	——	0.1520
Relative initial velocity	——	——	34.59	0.0003306	——	0.0004046
Error in initial relative velocity						
<10% relative position error						
%	1.590	0.7218	5.7752	0.9988	0.14870	0.1459
Initial position	79.521	36.097	152.38	26.372	7.5822	7.4395
Initial velocity	1.5954	0.72704	5.7754	0.99252	0.078734	0.027872
Relative initial position	26.655	12.100	152.38	43.073	1.4870	1.4590
Relative initial velocity	0.17172	0.081750	0.19974	0.0069359	0.0039152	0.0038834
Formation maintenance (<10 m)						
%	——	——	0.02650	0.02650	——	0.014600
Initial position	——	——	0.69919	0.69970	——	0.74446
Initial velocity	——	——	0.026501	0.026333	——	0.0027891
Relative initial position	——	——	0.69919	1.1428	——	0.14600
Relative initial velocity	——	——	0.000917	0.00018402	——	0.00038861

position and velocity conditions, Eqs. (6) and (7). The initial conditions are gradually altered by introducing a percentage error in the initial position or velocity, until the difference from motion in the zero-error case surpasses a specified limit. The maximum difference in the total relative position is determined by subtracting the total relative position in the original case from the total relative position in the slightly perturbed case, and finding the maximum over the propagated time span. The percentage difference in maximum total relative position is found by dividing that number by the maximum total relative position in the original case. The same can be done to determine sensitivity if the critical variable is the error in total velocity or a particular position or velocity component.

For some collinear libration point scenarios, and for the unrestricted and/or perturbed case of motion around the triangular points, sensitivity can be characterized by a loss of stability—a measure of the precision required to keep the spacecraft from spiraling away from the libration point. However, in the circular restricted three-body problem, the issue is not of stability loss but of the resurgence of the short- or long-period motion that had been filtered out by the analytical selection of initial conditions. Therefore this sensitivity analysis concentrates on maintaining the integrity of the formation, and the total distance between spacecraft, to within specific parameters. For each case, the required sensitivity is determined for a total relative position error of less than 10% over 30 days. In the case of the parallel formation, the analysis was also carried out for a desired relative out-of-plane ζ position of less than 10 m. For the leader–follower formation, the second constraint required that the maximum difference between the total absolute position of the first satellite at time $t + 1$ and of the second satellite at time t remains less than 10 m. For the case of the circular formation, the critical factor is ensuring that the total relative position stays nearly constant; the sensitivity is determined in terms of keeping less than 10 m deviation from the "perfect" case in total relative position. Results are shown in Table 3, first for the case of an error in initial position, and then for an error in initial velocity.

For the parallel formation, the formation maintenance constraint requires knowledge of the initial state to within 1000%, or 26 km and 1 m/ sec, indicating that changes in the initial relative state cause little departure from the parallel nature of the formation. The parallel formation thus appears to be the most robust of the formations designed here.

All of these sensitivity constraints are significantly smaller than the average errors between the modeled and simulated relative motion described above. This indicates that although the initial conditions are precise in each case, the model results do not fall within the desired small margin of error from the Swingby trajectories over the simulated time period. In most cases the required initial velocity knowledge is prohibitively small. Therefore, it seems unrealistic to constrain the precision to within the sensitivities indicated here; it would apparently be infeasible to design uncontrolled formations expecting less than a 10% relative position error over time at L_4.

IV. Perturbing Forces

The CR3BP is limited because it fails to account for the eccentricity of the lunar orbit, the gravitational effects of the sun and the other planets, oblateness of the Earth and the moon, solar radiation pressure, and many other smaller perturbations. In a 2004 paper, McLaughlin and Catlin [26] concluded that of the circular planar perturbing effects, the largest errors arise from neglecting the effects of solar gravity, followed by solar radiation pressure and the Earth's oblateness, in that order. This section contains a brief description of these effects and their consequences for libration point motion, as compared to the unperturbed case. For Swingby simulations, the time step for the Runge–Kutta–Nystrom propagation was 0.02 days; the 0.5 day step used in the CR3BP cases proved too inaccurate for perturbed models. Initial conditions are given for the short-period case in Table 1 (rotated to Swingby's coordinate frame) and propagated over 3 years.

A. Solar Gravity

The Earth–moon system cannot help but be affected by solar gravity. Though separated from the Earth and the moon by a distance of 1 astronomical unit (AU), the gravitational constant of the sun is 333,000 times that of the Earth, and the force and direction of the sun's gravitational pull on the system changes constantly as the Earth revolves around the sun while the moon revolves around the Earth.

To investigate the degree to which solar gravity affects relative motion at libration points, the short-period case was reevaluated in Swingby with all perturbing effects removed except the sun as a point mass. The Earth was also now modeled as traveling around the sun in

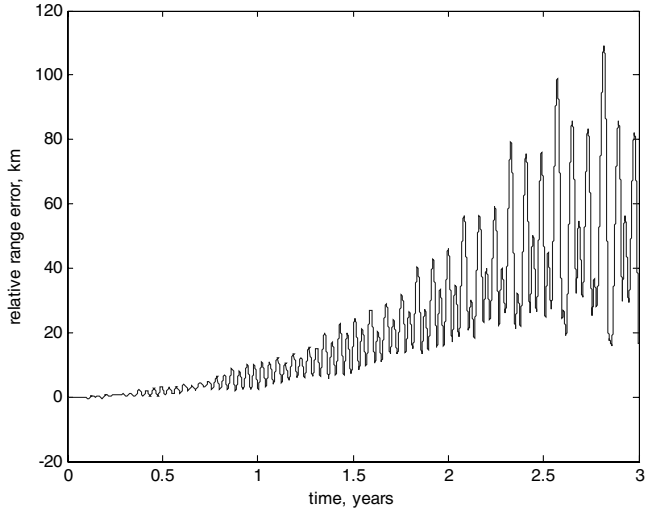

Fig. 12 Error in relative range caused by neglecting solar gravity for a short-period formation at L_4 over 3 years.

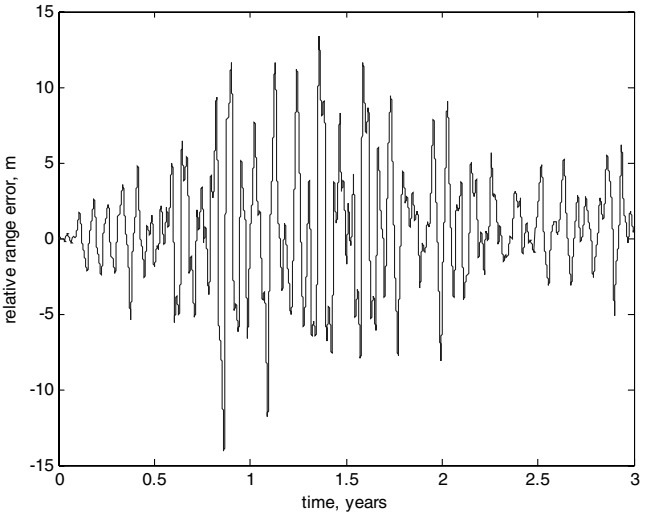

Fig. 13 Error in relative range caused by neglecting solar radiation pressure for a short-period formation at L_4 over 3 years.

a circular orbit at 1 AU, rather than fixed in space as assumed for the previous calculations. The results are compared to the zero-perturbation short-period case described earlier. The relative total position error caused by neglecting solar gravity reaches a peak of near 110 km at 2.82 years. A plot of the relative range error over time due to solar gravity is shown in Fig. 12. An approximately twice-monthly cycle corresponding to the lunar period is also visible.

Considering that the peak relative position for this scenario is only about 6 km in the unperturbed case, 2 orders of magnitude less than the approximately 1800% error, solar gravity clearly must be included in any model purporting to accurately reflect conditions within the Earth–moon system. Ideally, the effects of solar gravity should be modeled within the four-body problem. One difficulty is that the current CR3BP model of relative motion models spacecraft in circular equatorial orbits about the Earth; in this case the eccentricity and inclination are zero, and the right ascension of the ascending node and argument of perigee are undefined. An elliptical, inclined, restricted model could be employed instead, and in fact would remove additional sources of error from the original model. In this manner, some degree of model accuracy in solar gravity effects could be achieved without the complications of the four-body problem.

B. Solar Radiation Pressure

Photons emitted from the sun convey a force that, while small for each individual photon, becomes significant when distributed through many photons over the large area of a spacecraft. The force imparted depends on the solar flux (approximately 1367 W/m^2 near the Earth), the reflectivity of the spacecraft, its area facing the sun, and its position with respect to the sun. At lunar triangular points spacecraft are nearly always in sunlight, so periods of eclipse can be neglected.

To investigate the degree to which solar radiation pressure (SRP) affects relative motion at libration points, the short-period case was reevaluated in Swingby with all perturbing effects removed *except* solar radiation pressure. The sun was also present to provide direction to the incoming photons but did not gravitationally affect the system. The default spacecraft in Swingby, Clementine, was used; that model has a reflectivity coefficient of 1.2 and area facing the sun of 4.5 square meters. The results are compared to the zero-perturbation short-period case described earlier. The relative total position error caused by neglecting solar radiation reaches a peak of -14 m, or about 20%, at about 10 months. A plot of the relative range error over time due to solar radiation pressure is shown in Fig. 13.

This error is 3 orders of magnitude less than the peak relative distance in the unperturbed model. However, the required knowledge of initial conditions as derived from the sensitivity analysis is also on the meter level, and so SRP should not be excluded from investigations into real motion at the triangular points. Any errors mitigated by incorporation of SRP will be more than outweighed by the remaining errors due to neglecting solar gravity, so the SRP effect should not be examined exclusive of solar gravity if a significant increase in accuracy is desired. One must also consider the case of two spacecraft with differing areas perpendicular to the sun's radiation, or different ballistic coefficients; SRP would have a much larger relative perturbing effect in that scenario.

C. Earth Oblateness

Earth oblateness creates a nonuniform gravitational field in the planet's area of influence, which is often represented by a series of zonal harmonics based on a division of the globe into latitudinal slices of mass. Of these, the J_2, or first-order, effect is by far the largest, and has the greatest impact on spacecraft at L_4.

To investigate the degree to which first-order Earth oblateness affects relative motion at libration points, the short-period case was reevaluated in Swingby with all perturbing effects removed except the first-order zonal harmonic. The results are compared to the zero-perturbation short-period case described earlier. The relative total position error caused by neglecting Earth oblateness reaches a peak of near -1.5 mm, or less than 0.000025%, at about two months; this is an anomaly, however, as over the rest of the 3 years modeled, the error is never more than 0.35 mm.

This peak error is 6 orders of magnitude lower than any relative separation and 3 orders of magnitude lower than any initial precision required by all but the most stringently constrained systems. J_2 can be neglected for triangular libration point applications.

D. Stability

Stability of relative motion in the perturbed case is difficult to quantify; modeling for a time period longer than 3 years with a sufficiently small integration time step begins to take significant amounts of processor time. However, some broad conclusions can be drawn from the above error plots about the effect of adding perturbing forces to the ideally stable CR3BP case. Solar radiation pressure and Earth oblateness, despite an initial discontinuity in the latter case and some possible oscillation in the former, remain bounded over the entire 3 years. The solar gravity case, on the other hand, shows obvious and rapid growth after approximately six months. A Swingby simulation of absolute motion including all of the three most prominent perturbations over 10,000 days reveals an absolute trajectory that remains near the libration point for the first several months, then begins oscillating at a much larger amplitude than any of the other perturbed or unperturbed cases; but it seems clear that the spacecraft will continue to orbit the libration point indefinitely even under the influence of solar gravity. Therefore,

stability defined as the vehicle's tendency to remain in orbit about the libration point will not be an issue even in the perturbed system, at least for the initial conditions modeled here; although the dynamics modeled here represent relative motion, the dynamics of global motion are identically similar, and should remain stable to the same degree. For a definition of stability as a measure of proximity to the unperturbed case, a judicious application of minimal thrust repeated at intervals of a month would be sufficient to maintain the orbit to within set parameters, although additional work is needed to quantify the requirements.

V. Conclusions

The equations of relative motion derived herein and the formation flight models designed comprise a basic foundation for analytical modeling of relative motion at the Earth–moon triangular libration points. The analysis shows that formations are possible at the triangular points on uncontrolled trajectories, and additional scrutiny of these points is merited to further determine their applicability for mission design and support. The parallel and leader–follower formations, in particular, show great potential for applicability to future missions; the circular and projected circular, because they require additional simplification, do not apply to real-world scenarios unless the formations are actively controlled. However, the analysis presented here provides some guidelines for designing a somewhat analogous formation. These analytical descriptions of relative motion and formation flight designs provide a basis from which further formations can be developed using nonlinear techniques, in a comprehensible regime not limited by dependence on numerical integration techniques.

In conclusion, this research has provided a basic, analytical description of relative motion near the Earth–moon triangular libration points within the circular restricted three-body problem. Formations have been designed, compared to simulated numerical data with errors of less than 6% in all cases, and analyzed for sensitivity to initial conditions. Preliminary descriptions of the effects of perturbations have been provided. The solar gravity and radiation pressure forces were shown to be significant perturbations to the relative motion, but Earth oblateness was shown to be negligible. This analysis is a simple preliminary foundation to mission design and simulation and can be extended and applied in support of more complex descriptions of relative motion at the triangular points. The net product is a basic, analytical foundation for first-order relative dynamics at Earth–moon triangular points, confirming that the Earth–moon triangular points merit further study and should not be dismissed as potential locations for a future mission. The analysis serves as a basis and precursor for a more accurate and detailed mathematical description of relative motion at triangular libration points.

Moving outside of the Earth–moon system, the equations of relative motion presented herein are easily extended to libration points in other systems of two large masses, requiring only an alteration of the mass parameter. This analysis could be used to describe relative motion around triangular points within the sun–Earth system, or to model the dynamics of Trojan asteroids in the sun–Jupiter system. Indeed, these other instances are somewhat less perturbed than the Earth–moon case, as third-body gravitational effects are minimal and the orbits of the primaries are more nearly circular and less inclined than the orbit of the moon; a CR3BP description of relative motion is expected to prove closer to true motion in these cases than at Earth–moon triangular points.

Acknowledgments

This work was partially funded by a Graduate Student Researchers Program fellowship through the NASA Goddard Space Flight Center. The authors would like to thank Dave Folta, Richard Luquette, and Jesse Leitner of GSFC, for advice, access to Swingby software, and reference materials. Luquette served as NASA advisor for the fellowship. Chang-Hee Won and Stephen Johnson of the University of North Dakota served on the thesis advisory committee for the research and contributed significantly to its ultimate form. The UND Department of Space Studies is also appreciated for materials, office space, and constant support.

References

[1] Aldridge, E. C., Fiorina, C. S., Jackson, M. P., Leshin, L. A., Lyles, L. L., Spudis, P. D., deGrasse Tyson, N., Walker, R. S., and Zuber, M. T., "A Journey to Inspire, Innovate, and Discover: Report of the President's Commission on Implementation of United States Space Exploration Policy," U.S. Government Printing Office, Washington, D.C., 2004, pp. 28, 36.

[2] Farquhar, R. W., "The Flight of ISEE-3/ICE: Origins, Mission History, and a Legacy," *Journal of the Astronautical Sciences*, Vol. 49, No. 1, 2001, pp. 23–73.

[3] Lo, M. W., Williams, B. G., Bollman, W. E., Han, D., Hahn, Y., Bell, J. L., Hirst, E. A., Corwin, R. A., Hong, P. E., Howell, K. C., Barden, B., and Wilson, R., "Genesis Mission Design," *Journal of the Astronautical Sciences*, Vol. 49, No. 1, 2001, pp. 169–184.

[4] Farquhar, R. W., "Introduction," *Journal of the Astronautical Sciences*, Vol. 49, No. 1, 2001, pp. 1–9.

[5] Segerman, A. M., and Zedd, M. F., "Investigations of Spacecraft Orbits Around the L_2 Sun-Earth Libration Point—Part 2," Mathematics and Orbit Dynamics Section, Control Systems Branch, Spacecraft Engineering Department, Naval Center for Space Technology, Naval Research Laboratory, 2002.

[6] Collange, G., and Leitner, J., "Spacecraft Formation Design Near the Sun-Earth L_2 Point," AIAA Paper 2004-4781, Aug. 2004.

[7] Howell, K. C., and Marchand, B. G., "Natural and Non-Natural Spacecraft Formations Near the L1 and L2 Libration Points in the Sun-Earth/Moon Ephemeris System," *Dynamical Systems: An International Journal*, Vol. 20, No. 1, March 2005, pp. 149–173.

[8] Marchand, B. G., and Howell, K. C., "Control Strategies for Formation Flight in the Vicinity of Libration Points," *Journal of Guidance, Control, and Dynamics*, Vol. 28, No. 6, 2005, pp. 1210–1219.

[9] Vadali, S. R., Bae, H. W., and Alfriend, K. T., "Design and Control of Libration Point Satellite Formations," *Advances in the Astronautical Sciences*, Vol. 119, Univelt, San Diego, 2004, pp. 897–912.

[10] Luquette, R. J., and Sanner, R. M., "A Non-Linear Approach to Spacecraft Formation Control in the Vicinity of a Collinear Libration Point," *Advances in the Astronautical Sciences*, Vol. 109, Univelt, San Diego, 2001, pp. 437–446.

[11] Luquette, R. J., and Sanner, R. M., "Linear State-Space Representation of the Dynamics of Relative Motion Based on Restricted Three Body Dynamics," AIAA Paper 2004-4783, Aug. 2004.

[12] Luquette, R. J., Leitner, J., Gendreau, K., and Sanner, R. M., "Formation Control For The MAXIM Mission," *Proceedings of the 2nd International Symposium on Formation Flying Missions and Technologies* [CD-ROM], Washington, D.C., NASA CP-2005-212781, 14–16 Sept. 2004.

[13] Michael, W. H., "Considerations of the Motion of a Small Body in the Vicinity of the Stable Libration Points of the Earth-Moon System," NASA TR-160, 1963.

[14] Szebehely, V., *Theory of Orbits: The Restricted Problem of Three Bodies*, Academic Press, Orlando, 1967.

[15] Rand, R., and Podgorski, W., "Geometrical Dynamics: A New Approach to Periodic Orbits around L_4," *Celestial Mechanics*, Vol. 6, No. 4, 1972, pp. 416–420.

[16] Blackburn, J. A., Nerenbergy, M. A. H., and Beaudoin, Y., "Satellite Motion in the Vicinity of the Triangular Libration Points," *American Journal of Physics*, Vol. 45, No. 11, 1977, pp. 1077–1081.

[17] McKenzie, R., and Szebehely, V., "Non-Linear Stability Around the Triangular Libration Points," *Celestial Mechanics*, Vol. 23, No. 3, 1981, pp. 223–229.

[18] Szebehely, V., "Theory and Application of Motion Around Equilibrium Points," *Methods in Astrodynamics and Celestial Mechanics*, edited by R. L. Duncombe, and V. G. Szebehely, Progress in Astronautics and Aeronautics, Vol. 17, Academic Press, New York, 1966, pp. 3–30.

[19] Danby, J. M. A., "Inclusion of Extra Forces in the Problem of Three Bodies," *Astronomical Journal*, Vol. 70, No. 3, 1965, pp. 181–189.

[20] Breakwell, J. V., and Pringle, R., Jr., "Resonances Affecting Motion Near the Earth-Moon Equilateral Libration Points," *Methods in Astrodynamics and Celestial Mechanics*, edited by R. L. Duncombe, and V. G. Szebehely, Progress in Astronautics and Aeronautics, Vol. 17, Academic Press, New York, 1966, pp. 55–74.

[21] Gurfil, P., and Kasdin, N. J., "Stability and Control of Spacecraft Formation Flying in Trajectories of the Restricted Three-Body Problem," *Acta Astronautica*, Vol. 54, No. 6, 2004, pp. 433–453.

[22] Gómez, G., Llibre, J., Martinez, R., and Simó, C., *World Scientific Monograph Series in Mathematics—Vol. 3: Dynamics and Mission Design Near Libration Points: Vol. II Fundamentals: The Case of Triangular Libration Points*, World Scientific Publishing, Singapore, 2000.

[23] Gómez, G., Jorba, À., Masdemont, J., and Simó, C., *World Scientific Monograph Series in Mathematics—Vol. 5: Dynamics and Mission Design Near Libration Points: Vol. IV Advanced Methods for Triangular Points*, World Scientific Publishing, Singapore, 2001.

[24] Catlin, K., and McLaughlin, C. A., "Relative Motion of Two Spacecraft Near the Earth-Moon Triangular Libration Points," AIAA Paper 2004-4743, Aug. 2004.

[25] Dunham, D. W., and Muhonen, D. P., "Tables of Libration-Point Parameters for Selected Solar System Objects," *Journal of the Astronautical Sciences*, Vol. 49, No. 1, 2001, pp. 197–217.

[26] McLaughlin, C. A., and Catlin, K., "Perturbation Analysis for Spacecraft Formations Near the Earth-Moon Triangular Libration Points," *Proceedings of the 2nd International Symposium on Formation Flying Missions and Technologies* [CD-ROM], Washington, D.C., NASA CP-2005-212781, 14–16 Sept. 2004.

D. Spencer
Associate Editor